Solar Energy Materials and Solar Cells 173 (2017) 128–133

Contents lists available at ScienceDirect

Solar Energy Materials and Solar Cells

journal homepage: www.elsevier.com/locate/solmat

The concept of skins for silicon solar cell modeling

Andreas Fell[a,*], Jonas Schön[a], Martin C. Schubert[a], Stefan W. Glunz[a,b]

[a] Fraunhofer Institute for Solar Energy Systems (ISE), Heidenhofstrasse 2, 79110 Freiburg, Germany
[b] Department of Sustainable Systems Engineering, Albert Ludwig University of Freiburg, Georges-Köhler-Allee 103, D-79110 Freiburg, Germany

ARTICLE INFO

Keywords:
Silicon solar cells
Device modeling
Device simulation
Quokka
Skin
Multiscale modeling
Conductive boundary

ABSTRACT

Within (crystalline silicon) solar cell modeling, a skin means the *thin* region from the quasi-neutral bulk to the actual surface or metal contact, including e.g. doping profiles, induced band-bending or top-cells of a tandem configuration. A typical highly doped skin is commonly characterized by its main lumped properties: effective recombination via $J_{0,skin}$ and lateral conductance via R_{sheet}. When applied as a boundary condition to bulk carrier transport modeling, it is known as the conductive boundary model. However, the detailed resolution of physics inside the skin is then lacking but required in many cases, and possible complexities, like injection dependence of the lumped parameters, are commonly neglected. This work introduces a general parameterization of skins, which accounts fully for injection dependence and a vertical resistance, and is thus able to accurately describe arbitrarily complex skins by lumped parameters. A "skin solver" is implemented in the solar cell simulation software Quokka3 to solve a detailed skin in 1D and to perform the general parameterization. Additionally, the performance of the multidimensional quasi-neutral bulk (qn-bulk) solver is largely improved compared to Quokka2, enabling, for the first time, the 3D discretization and solution of up to an entire 156 mm × 156 mm solar cell in manageable computing times. Quokka3 can then consistently couple the skin solver with the qn-bulk solver. With this multiscale modeling approach, the user can define and solve a solar cell device including the details of the skins orders of magnitude faster compared to generic device simulation software, without loss of accuracy for the majority of conditions in wafer-based silicon solar cells. The new capabilities are demonstrated by showing how the front phosphorus diffusion of a PERC solar cell can be optimized with unprecedented completeness and accuracy. Besides accurately modeling 3D current transport in the bulk, the single solution domain intrinsically accounts for the busbar influence (both recombination and shading), the distributed resistance of the fingers, and the limited current collection independent of the surface area enlargement by texturing.

1. Introduction

When modeling crystalline silicon solar cells, three main regions of the device can be distinguished: a) the quasi-neutral and lowly doped bulk, which is relatively thick and acts as the main photon absorber, b) the skins [1], which are the thin near-surface regions selectively conducting electrons or holes to the metal contacts (laterally and vertically), and c) the metal grid. While current transport in the (quasi-neutral) bulk and the metal is relatively easy to model, the skins contain more challenging physics like for example high doping density with strong gradients, a space-charge region, induced band bending, multiple material layers etc.. It is therefore popular to describe a skin by its lumped properties, typically by an effective recombination property $J_{0,skin}$, and sheet resistance R_{sheet}. Those lumped properties, which are usually well measurable, can be used as a boundary condition when solving bulk carrier transport, greatly simplifying the modeling and thus enhancing speed for numerical solvers [2]. This approach is known as the conductive boundary model [3].

Often the detailed physics within the skin are of interest and need to be modeled, e.g. when investigating the impact of changes in the doping profile. This task is readily available in 1D by various (free) software tools. Multidimensional detailed modeling is however restricted to powerful commercial semiconductor simulation software, with drawbacks of significant user effort and much larger computational demand compared to lumped skin modeling.

A way to reduce the high effort for detailed cell modeling is to employ a three-step approach: 1) for each skin solve their characteristics in 1D, 2) determine their lumped properties, 3) apply these properties as boundary conditions for solving bulk carrier transport. Such a *multiscale* approach was shown to greatly improve speed of 1D cell simulations in [4]. For 2D/3D simulations one can combine different software tools, e.g. using EDNA2 [5,6] to determine the skin's

* Corresponding author.
E-mail address: andreas.fell@ise.fraunhofer.de (A. Fell).

http://dx.doi.org/10.1016/j.solmat.2017.05.012
Received 31 March 2017; Received in revised form 29 April 2017; Accepted 7 May 2017
Available online 21 May 2017

$J_{0,skin}$ and R_{sheet} as inputs for Quokka2 [2]. However, limitations of this approach are:

- Injection dependence of the recombination is complicated to account for, and thus usually neglected
- Vertical potential difference within the skin is neglected (e.g. from thin insulator layer or space-charge-region)
- Difficulty to consistently account for non-ideal collection of carriers within the skin, i.e. the skin's collection efficiency
- Prone to systematic mistakes due to using different tools (e.g. inconsistent $n_{i,eff}$ model, inconsistency of generation profile and skin depth)

This work alleviates those limitations by a) introducing a generally valid parameterization of the skin characteristics, and b) implementing both a 1D detailed "skin solver" and the multidimensional bulk solver in a single software tool, namely Quokka3. Notably, Quokka3 can handle multiple (full-area or local) skin features. They can individually be defined either by lumped inputs or by detailed inputs for the multiscale approach, allowing the user the option to choose just the right level of detail for a specific modeling task.

2. General skin parameterization

From a multidimensional numerical modeling perspective, a lumped skin is treated as a single-element-deep surface mesh, see Fig. 1. When using quasi-Fermi potentials as solution variables, as is the case in Quokka, the quasi-neutral steady-state solver requires a unique relationship between all face potentials and the face currents. That is, the element can be viewed as a black-box electrical circuit, which holds regardless of the details of the physics happening within the skin. The only assumption is that for significant lateral transport relative to the bulk, the majority carrier potential φ_{skin} is assumed to be constant within the main conductive region of the skin. This is the case e.g. within a highly doped near-surface region, or within the transparent conductive oxide (TCO) layer in a hetero-junction cell design. The assumption generally holds well for most typical crystalline silicon solar cell skins, in particular because of typical skins being *thin*, as can be perceived by the following:

- The assumption of a uniform φ_{skin} is only important for lateral current transport: for an effectively non-conductive skin, φ_{skin} denotes the potential only at the actual surface.
- To achieve significant lateral conductance, the vertical conductance of a thin region becomes very high, prohibiting significant vertical potential gradients.
- Most commonly only one type of carrier can have a significant lateral conductance within the skin, meaning that the skin can be assumed either purely *n*-type, *p*-type or non-conductive (neglecting some special cases, e.g. a "buried emitter").

For parameterizing the black-box characteristics, an equivalent

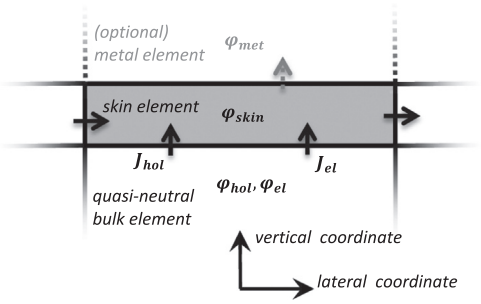

Fig. 1. Sketch of a single skin element within a 2D discretization for a numerical solver.

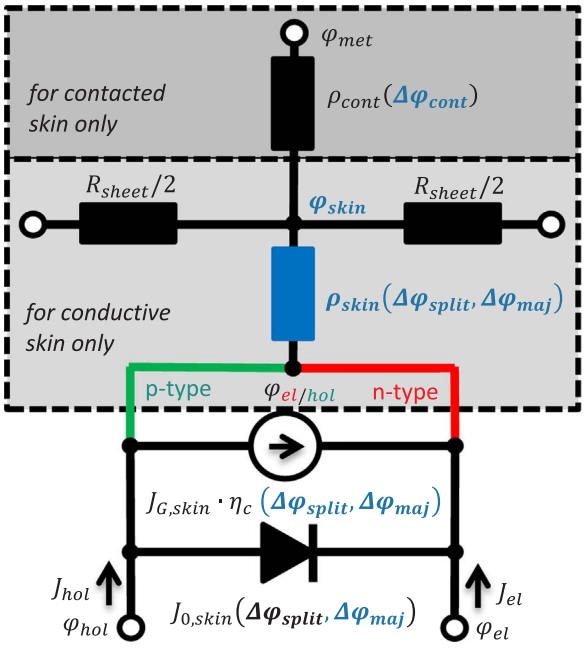

Fig. 2. Equivalent circuit model for a skin element; blue colour indicates the extensions to the conductive boundary model, accounting for vertical resistance and potential dependence of all parameters.

circuit model is applied, see Fig. 2. It extends the conductive boundary model by a) adding a vertical resistance ρ_{skin} between the bulk and the skin, and b) adding full potential-dependence (i.e. injection dependence) to all parameters. With the further assumption of being able to superimpose vertical and lateral current transport, which holds well for the same reasons given above, the main parameters are generally dependent on two potential differences only: i) the bulk-side quasi-Fermi potential split $\Delta\varphi_{split} = \varphi_{el} - \varphi_{hol}$, and ii) the vertical majority carrier potential difference $\Delta\varphi_{maj} = \varphi_{skin} - \varphi_{maj}$. For contacted skins, the additional metal contact resistivity ρ_{cont} depends (only) on the metal contact potential difference $\Delta\varphi_{cont} = \varphi_{met} - \varphi_{skin}$.

Generation of carriers within the skin is accounted for by the generation current density $J_{G,skin}$. Although not necessary from the black-box perspective, the lumped parameters become more meaningful if the skins's collection efficiency η_c is applied to $J_{G,skin}$. This way the recombination of carriers being generated within the skin is separated from the recombination of bulk-side carriers defined via $J_{0,skin}$, which enables a better definition of a texture multiplier as discussed in Section 3.3.

Note that while these lumped parameters are not always physically meaningful, they are generally valid as parameters also for arbitrarily complex skins. For example, ρ_{skin} can become negative to account for the voltage from a thin top-cell in a tandem configuration.

3. Implementation in Quokka3

3.1. Improved multidimensional quasi-neutral bulk (qn-bulk) solver

For solving multidimensional carrier transport in the bulk, the same efficient model as in Quokka2 is implemented, which most notably uses the quasi-neutrality assumption for omitting the need to solve the Poisson equation [2]. This model has been successfully validated to be accurate for typical silicon solar cells by comparisons against full detailed semiconductor device simulations [7,8]. In addition to Quokka2, which applies the common conductive boundary approach, Quokka3 enhances the qn-bulk solver by: i) a large performance boost via a rebuild in C++ and using PETSC [9] as a state-of-the-art library to solve the resulting system of nonlinear equations, ii) including an additional conductive layer on top of the skin layer at the front and rear

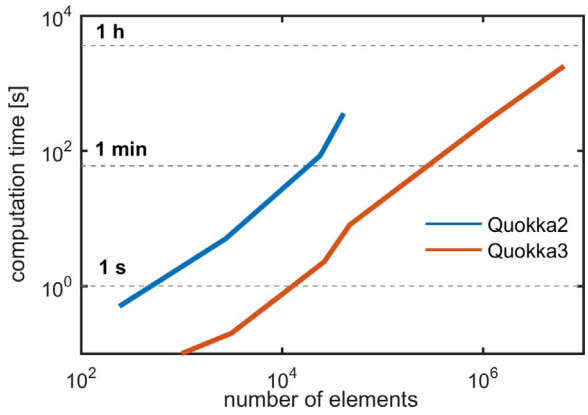

Fig. 3. Computation time (single voltage) of different mesh sizes for the different Quokka builds on consumer-grade hardware.

side to solve current transport in the metal layer, iii) supporting the general skin parameterization of this work as a boundary condition, and iv) supporting the definition of arbitrary skin, metal and contact feature geometries (via multiple rectangular features).

In Fig. 3 the computation time of arbitrary simulation setups is shown as a function of mesh size for Quokka2 (Matlab) and Quokka3 (C++/ PETSC). It can be seen that Quokka3 largely outperforms Quokka2. Due to less required elements compared to full detailed multidimensional device simulation of the same geometry, Quokka3 has the capability to solve unprecedented large geometries in a single solution domain. Computation times even for full-area cells are still manageable, ranging from ~hour (e.g. simple Al-BSF cell, ~1 million elements) to several hours (e.g. PERC cell with line rear contacts > 5 million elements) and beyond for more complex geometries (IBC cell, …). On the "low end", common unit cell geometries (~100 to ~10 k elements) are solved in sub-seconds to seconds. Notably, the solution times for a given number of elements is similar to commercial state-of-the-art numerical solvers.

3.2. Skin solver

Quokka3 features another basic solver besides its qn-bulk solver, which solves the full semiconductor equations, i.e. including the Poisson equation, in 1D using an equivalent finite-differences approach. The "1D detailed solver" employs up-to-date material models comprising Fermi-Dirac statistics, doping- and injection-dependent band-gap-narrowing models [10–12] and incomplete ionization [13]. As boundary conditions, both ideal (flat-band) electron or hole contacts, as well as Schottky-type contacts are supported.

The 1D detailed solver can be applied either to a cell domain, where it essentially replicates PC1D functionality, or to a skin domain, which is the focus of this work. Main difference to the cell domain is that on one side, instead of a contact, a quasi-neutral boundary condition is applied. It defines the quasi-Fermi potential split $\Delta\varphi_{split}$ and the majority potential difference to the opposite boundary $\Delta\varphi_{maj}$, matching the general skin parameterization. For non-contacted skins, a virtual ideal contact with the respective type is applied (electron contact on n-type skin, hole contact on p-type skin), which represents lateral current extraction.

Once a solution for a defined set of boundary potentials has been found, the results are parameterized in the following way (assuming an illuminated skin, i.e. with generation):

- R_{sheet} is the inverse of the integral conductivity; this is evaluated for both carrier types, and the lower R_{sheet} value determines the majority carrier type of the skin.
- $J_{G,skin}$ is determined by integrating the generation rate.
- The skin potential φ_{skin} is assigned the majority potential of the element with the highest majority carrier conductivity (usually the surface element).
- The vertical resistance ρ_{skin} is calculated by the difference of the skin potential and the bulk-side majority carrier quasi-Fermi potential over the net current density.
- The total recombination current density $J_{rec,light}$ is determined by integrating volume recombination and adding interface recombination.
- Then generation is switched off and a second simulation is performed.
- The total recombination current density $J_{rec,dark}$ is determined by integrating volume recombination and adding interface recombination (which (only) in the dark equals the minority carrier current density through the bulk-side boundary).
- Any additional recombination in the illuminated case compared to the dark case is attributed to carriers generated within the skin, so that the collection efficiency η_c is defined as $1-(J_{rec,light} - J_{rec,dark})/J_{G,skin}$.
- Consistent with above, $J_{0,skin}$ for both the illuminated and dark case is defined as $J_{rec,dark}/\left[\exp\left(\frac{\Delta\varphi_{split}}{V_t}\right)-1\right]$, where V_t denotes the thermal voltage.

To validate the new skin solver, the $J_{0,skin}$ values from two recent publications are successfully reproduced (see Fig. 4): a) varying phosphorus and boron doping profiles simulated with Sentaurus Device, EDNA2 and cmd-PC1D [14], b) several phosphorus doping profiles accounting for phosphorus precipitates recombination simulated with Sentaurus Device [15].

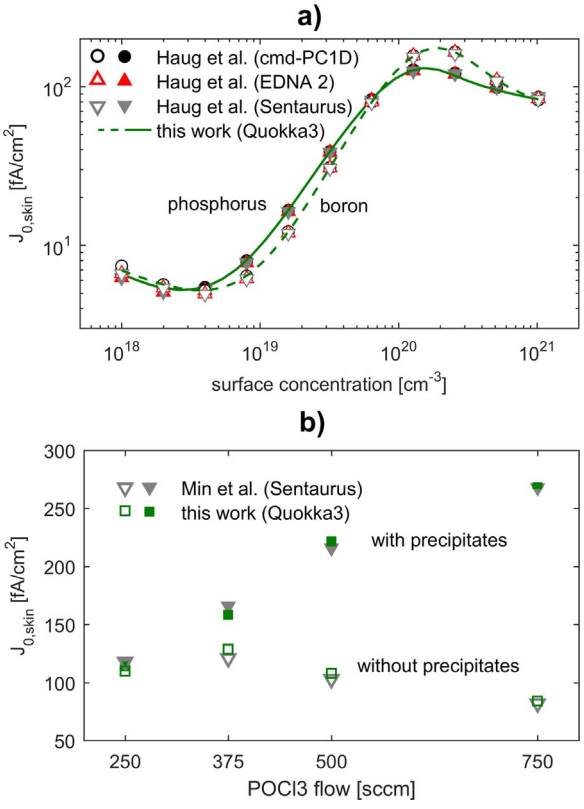

Fig. 4. Comparison of $J_{0,skin}$ values with other simulation tools; a) input from [14] for both n-type / phosphorus doping (*solid line, filled symbols*) and p-type / boron doping (*dashed line, open symbol*); b) input from [15] with (*filled symbols*) and without (*open symbols*) considering phosphorus precipitate recombination.

3.3. Multiscale modeling

As described in the introduction, multiscale modeling means that one or more skins are defined by detailed (not lumped) inputs, solved in 1D, parameterized, and coupled to the qn-bulk solver as boundary conditions. The main advantage is a vastly improved computational speed, while not compromising accuracy when using the general skin parameterization.

As a first step, a skin depth needs to be defined, to define which part of the device belongs to the skin or the bulk, respectively. The exact position is hereby not very important, as long as quasi-neutrality does hold at the split position and the resulting skin depth is thin. Quokka3 can either guess a suitable skin depth based on doping profile inputs, or take it as a user input.

An important advantage of performing the multiscale modeling regards consistent optical modeling, which would be difficult to ensure with separate software tools. This is straightforward when using a generation profile as an input. For spectrally resolved optical modeling, the "T_{ext}-Z" model [16] can be used, which enables e.g. consistent quantum-efficiency modeling within the multiscale approach. The consistency is particularly important to correctly account for current collection within the skins, i.e. for η_c.

Another relevant advantage compared to full detailed device modeling exists for the common case of a textured surface being approximated by a planar solution domain. In full detailed modeling a texture multiplier is commonly applied to represent increased recombination due to the surface area enlargement. It is however only possible to increase the entire skin recombination, typically via the surface recombination parameters, which then unavoidably leads to an unphysical underestimation of the current collection in the skin [8]. In the multiscale approach, a texture multiplier can be applied solely to the bulk side recombination. As recombination of carriers generated within the skin are accounted for by η_c and recombination of carriers generated within the bulk are exclusively accounted for by $J_{0,skin}$, the texture multiplier is applied only to the latter.

Quokka3 implements 3 different modes to couple the skin solver with the qn-bulk solver, which can be set individually for each detailed skin:

- *single point*: the skin is solved once only for a defined set of potentials to derive constant values for the skin parameters. This requires the least computational effort, und is valid for typical skins including high doping or high charge.
- *injection dependent*: the skin is solved for the relevant range of quasi-Fermi level splits, but at a constant majority potential difference. This is best for skins which do show significant injection-dependent recombination but low (or constant) vertical resistance (e.g. passivation with moderate charge)
- *full coupling*: the skin is solved for the full relevant range of the quasi-Fermi level split and the majority potential difference. While costlier in terms of computational demand, this is the generally valid approach for any skin properties.

Regarding numerical performance, it is noted that the effort to solve the skins scales essentially with the number of skins, while the effort to solve the bulk scales with the number of mesh elements. That means that for small geometries, e.g. 2D unit cells, the overall solution time might well be limited by solving the skins, which is however still in the order of sub-seconds to a maximum of minutes for full coupling. For larger geometries with solution times of the qn-bulk solver above ~minutes, the multiscale modeling does not add significantly to the overall solution time.

4. PERC phosphorus doping profile optimization

As an application example highlighting the usefulness of the multi-scale modeling approach, the front phosphorus doping profile of an industry-typical PERC cell is optimized. The input parameter set for the PERC cell given in [8] is used as the reference case. The doping profile is varied by employing a Gaussian profile with varying depth factor (standard deviation) and surface concentration. To render the profiles somewhat representative for industrial relevant ones, inactive phosphorus is accounted for via the incomplete ionization model presented in [13] and additionally via a solubility limit of $2.5{\bullet}10^{20} cm^{-3}$. The inactive phosphorus then results in additional SRH recombination with the parameters presented in [15]. The surface recombination velocity is defined as a function of total surface concentration according to the parameterization presented in [15]. In Fig. 5 selected profiles are plotted. To account for the texture, a texture multiplier with a typical value of 1.2 [17] is applied to the $J_{0,skin}$, which importantly does not reduce the collection efficiency and thus the current density, as discussed above. Note that the rear side skins, which are not to be optimized, are modeled by their lumped properties for simplicity and speed.

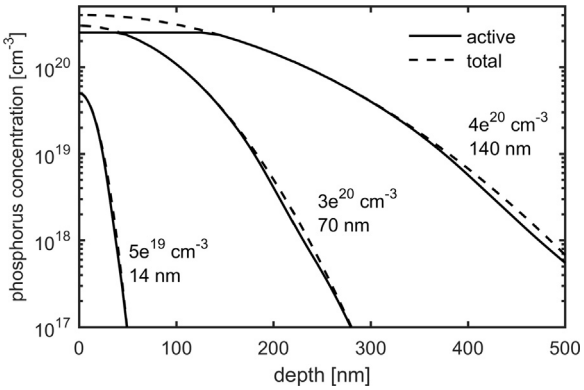

Fig. 5. Selected doping profiles featuring a Gaussian shape and inactive phosphorus, for three different pairs of surface concentration and standard deviation.

When changing the doping profile, it is important to note that this also impacts the optimum front finger pitch. That means that for a fair optimization, for each individual profile the pitch has to be optimized. This is not trivial in common unit-cell PERC modeling, as the front and rear pitch cannot be set independently, and is therefore often disregarded and considered in a separate modeling approach. With the numerical performance of Quokka3 however, it becomes feasible to (almost) arbitrarily set the front and rear pitch, where Quokka3 finds the least common multiplier of the half-pitches and constructs a single domain for the actual symmetry element. Obviously, care has to be taken that the domain does not become extremely large for arbitrary pitch values. However, as up to a full cell can be defined, there is no limitation to model experimentally realizable grid geometries. Here, for a constant rear contact pitch of $0.85mm$, simulations are performed for front finger pitch values of $1.02mm$, $1.19mm$, $1.36mm$, $1.7mm$ and $2.04mm$, and the result with highest efficiency is taken as the optimum point for a specific profile. Note that also the front finger pitch of the reference cell is optimized this way, as in [8] it was set to double the rear pitch for simplicity, resulting in an reference efficiency of 20.9%.

Furthermore, the chosen solution domain includes the busbar, and consequently half a finger length (=half busbar pitch) to represent a "busbar enhanced" symmetry element. This not only accurately accounts for localized shading and recombination of the busbar, but also intrinsically accounts for the distributed resistive finger loss without the need to separately calculate a series resistance value. The resulting solution domains are shown in Fig. 6.

In Fig. 7 the results are summarized, with a computation time of simulating the ~300 JV-curves of around one hour. The maximum efficiency of 21.5% identifies moderate room for improving the doping profile for an efficiency increase of 0.6%abs. It can also be seen that the current density variation, caused by the varying collection efficiency, is

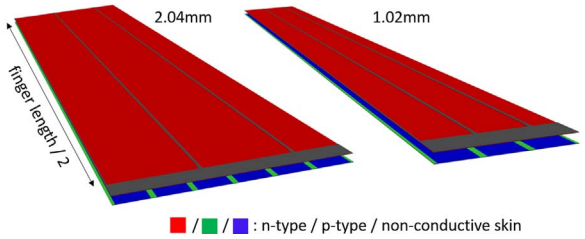

Fig. 6. "Busbar enhanced" symmetry elements for the lowest and largest front finger pitch as used for the n-type doping profile optimization.

very significant, highlighting the importance of applying a meaningful texture multiplier. The overall optimum tends to be at highly doped but thin profiles, which is consistent with common understanding.

5. Conclusions

This work discussed the concept of modeling skins as distinctive regions separately to the quasi-neutral bulk within (silicon) solar cell modeling, which forms the conceptual backbone of the solar cell simulation software Quokka3. Here two different solvers account for the two different regions:

qn-bulk solver: a multidimensional quasi-neutral bulk solver employing skins as lumped boundary conditions. It's rebuild in C++ comes with a numerical performance increase of up to two orders of magnitude compared to the implementation in Quokka2, and is capable of solving large geometries up to full 156 mm cells in 3D. It further extends the conductive-boundary implementation in Quokka2 by i) allowing generic geometry definition, ii) allowing features to be placed on edges (e.g. for edge recombination), iii) allowing a general skin parameterization to be applied as a boundary condition and iv) including an additional metal layer and thus accurately accounting for distributed metal grid resistance.

Skin solver: a one-dimensional detailed physics solver including Poisson equation, i.e. non-charge-neutral effects, which can be applied to a skin using a quasi-neutral boundary condition at the bulk-side. It can solve a detailed skin and perform the general parameterization presented in this work. The skin solver was successfully validated against state-of-the-art device simulation tools.

The multiscale approach employed by Quokka3 was described, wherein the skin solver is consistently coupled to the qn-bulk solver. This has the following main benefits compared to the "brute-force" way of using full detailed modeling for the entire domain:

- Vastly improved speed, practically enabling much larger solution domains to be solved.
- Within a single simulation, different skins can individually be described optionally by lumped inputs or detailed inputs.
- When approximating a textured surface by a planar solution domain, a texture multiplier can be applied exclusively to bulk-side recombination without affecting the short-wavelength collection efficiency.

Being valid for most cases of interest in modeling wafer-based silicon solar cells, the concept only breaks when non-quasi-neutral multidimensional effects become relevant, that is e.g. when trying to resolve a single contact spike, or the volumetric shape of a local back surface field.

The enhanced capabilities of Quokka3 were showcased by optimizing the doping profile of a front phosphorus diffusion within a PERC cell design with unprecedented completeness of relevant effects. The

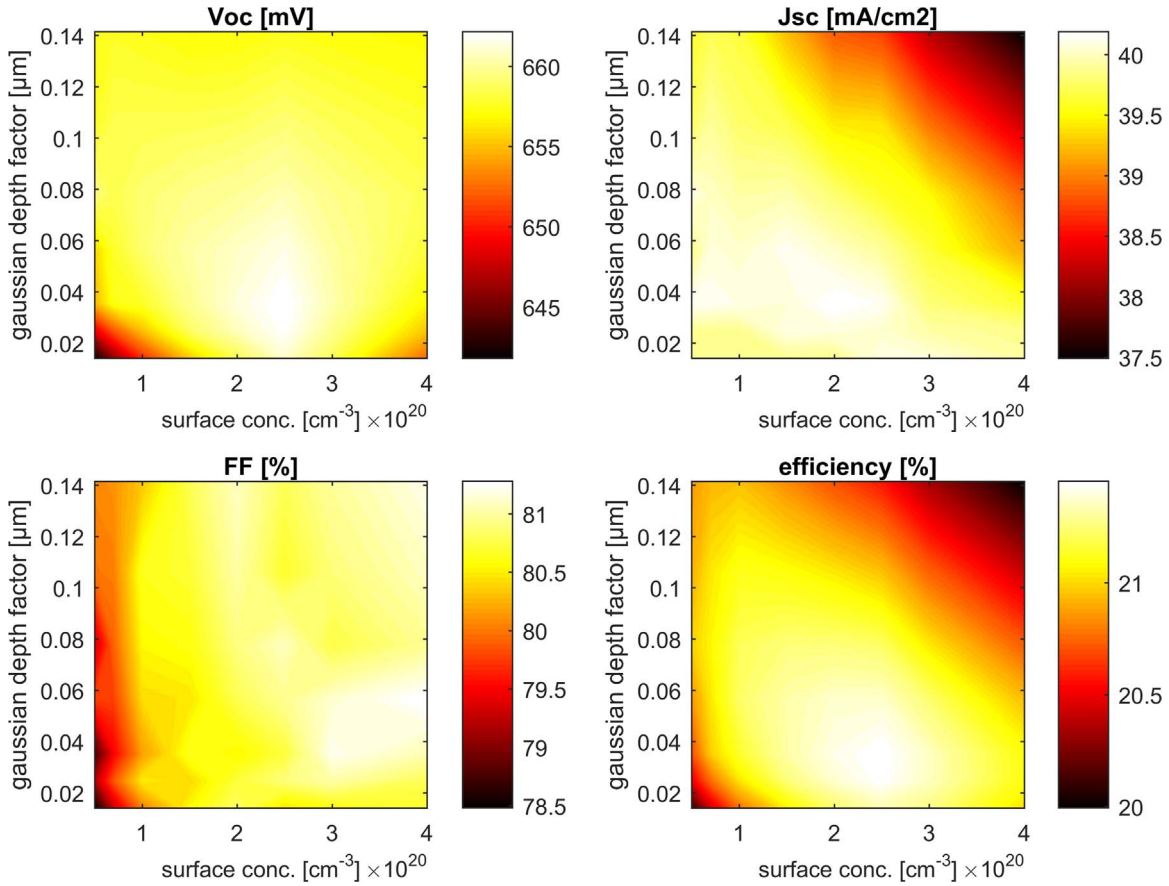

Fig. 7. Light current-voltage curve parameters for the investigated range of emitter profiles; each data point is given for the optimum pitch regarding efficiency. Some patchiness is caused by the discrete pitch variation.

particular effects considered accurately within the single symmetry element including the busbar and half a finger length are: i) 3D carrier transport in the bulk, ii) localized recombination and shading of busbars, iii) distributed finger resistance, iv) optimization of the front finger pitch for constant rear contact pitch and v) non-ideal current collection within the front skin not affected by the texture multiplier applied to bulk-side recombination.

With those capabilities being readily accessible within a single software tool, this is envisaged to impact the silicon PV community through increasing the completeness and efficacy of standard solar cell simulations.

Acknowledgements

The authors would like to thank Halvard Haug and Byungsul Min for providing the data for the skin solver validation.

Funding: This work was supported by the European Commission through the Marie-Curie individual fellowship “Quokka maturation”.

References

[1] A. Cuevas, T. Allen, J. Bullock, Y. Wan, X. Zhang, Skin care for healthy silicon solar cells, in *42nd IEEE PVSEC*, pp. 1–6.
[2] A. Fell, A free and fast three-dimensional/two-dimensional solar cell simulator featuring conductive boundary and quasi-neutrality approximations, IEEE Trans. Electron Devices 60 (2) (2013) 733–738.
[3] R. Brendel, Modeling solar cells with the dopant-diffused layers treated as conductive boundaries, Progress. Photovolt.: Res. Appl. 20 (1) (2012) 31–43.
[4] K.R. McIntosh, M.D. Abbott, Fast and accurate 1D cell simulation, in *31st EUPVSEC*, pp. 489–494.
[5] K.R. McIntosh, P.P. Altermatt, A freeware 1D emitter model for silicon solar cells, in: Proceedings of the 35th IEEE Photovoltaic Specialists Conference PVSC, pp. 2188–2193.
[6] K.R. McIntosh *et al.*, An examination of three common assumption used to simulate recombination in heavily doped silicon, in: Proceedings of the 28th European Photovoltaic Solar Energy Conference and Exhibition, pp. 1672–1679.
[7] A. Fell, K.C. Fong, K.R. McIntosh, E. Franklin, A.W. Blakers, 3-D Simulation of Interdigitated-Back-Contact silicon solar cells with quokka including perimeter losses, IEEE J. Photovolt. 4 (4) (2014) 1040–1045.
[8] A. Fell, et al., Input parameters for the simulation of silicon solar cells in 2014, IEEE J. Photovolt. 5 (4) (2015) 1250–1263.
[9] S. Balay, *et al., PETSc web page,*, 2016.
[10] A. Schenk, Finite-temperature full random-phase approximation model of band gap narrowing for silicon device simulation, J. Appl. Phys. 84 (7) (1998) 3684–3695.
[11] Di Yan, A. Cuevas, Empirical determination of the energy band gap narrowing in highly doped n+ silicon, J. Appl. Phys. 114 (4) (2013) 44508.
[12] Di Yan, A. Cuevas, Empirical determination of the energy band gap narrowing in p + silicon heavily doped with boron, J. Appl. Phys. 116 (19) (2014) 194505.
[13] P.P. Altermatt, A. Schenk, G. Heiser, A simulation model for the density of states and for incomplete ionization in crystalline silicon. I. Establishing the model in Si: P, J. Appl. Phys. 100 (11) (2006) 113714.
[14] H. Haug, A. Kimmerle, J. Greulich, A. Wolf, E. Stensrud Marstein, Implementation of Fermi–Dirac statistics and advanced models in PC1D for precise simulations of silicon solar cells, Sol. Energy Mater. Sol. Cells 131 (0) (2014) 30–36.
[15] B. Min, et al., Heavily doped Si: P emitters of crystalline Si solar cells: recombination due to phosphorus precipitation, Phys. Status Solidi (RRL)-Rapid Res. Lett. 8 (2014) 680–684.
[16] A. Fell, K.R. McIntosh, K.C. Fong, Simplified device simulation of silicon solar cells using a lumped parameter optical model, IEEE J. Photovolt. (2016) 1–6.
[17] S.C. Baker-Finch, K.R. McIntosh, M.L. Terry, Y. Wan, Isotextured silicon solar cell analysis and modeling 2: recombination and device modeling, IEEE J. Photovolt. 2 (4) (2012) 465–472.